geotechnics

MDPI

Article

Strength Mobilisation in Karlsruhe Fine Sand

Jinghong Liu, Yi Pik Cheng *, and Min Deng *

Department of Civil, Environmental, and Geomatic Engineering, University College London, Gower Steet, London WC1E 6BT, UK; jinghong.liu.20@alumni.ucl.ac.uk

* Correspondence: yi.cheng@ucl.ac.uk (Y.P.C.); min.deng@ucl.ac.uk (M.D.)

Abstract: The strength mobilisation framework was adopted for the first time to describe the stress–strain responses for three different types of sands, including a total of 30 published drained triaxial tests—25 for Karlsruhe Fine Sand, 2 for Ottawa sands and 3 for Fontainebleau sand, under confining pressures ranging from 50 to 400 kPa. The peak shear strength τ_{peak} obtained from drained triaxial shearing of these sands was used to normalise shear stress. Shear strains normalised at peak strength γ_{peak} and at half peak of shear strength $\gamma_{M=2}$ were taken as the normalised reference strains, and the results were compared. Power–law functions were then derived when the mobilised strength was between $0.2\tau_{peak}$ and $0.8\tau_{peak}$. Exponents of the power–law functions of these sands were found to be lower than in the published undrained shearing data of clays. Using $\gamma_{M=2}$ as the reference strain shows a slightly better power–law correlation than using γ_{peak}. Linear relationships between the reference strains and variables, such as relative density, relative dilatancy index, and dilatancy, are identified.

Keywords: sands; strength mobilisation; power law; stress–strain response

1. Introduction

Soils are natural materials formed by the chemical or physical weathering of rocks. Soils are complex porous materials; soils obtained from different regions show a wide range of properties (e.g., density, void ratio, particle shape, and grain size distribution). Not only do the physical properties of soil particles such as particle size and composition vary, but site conditions such as confining stress range, and drainage conditions also have significant impacts on its mechanical behaviour. When a soil is subjected to external load, its deformations show non-linear elastoplastic characteristics in both volumetric and shear domains. Traditional geotechnical design calculations using the concept of safety factors, however, could only consider ultimate stresses but ignore deformation despite its significant impact on the performance of soil structures. To predict the stress–strain–volume behaviour of soils, geotechnical engineers have proposed a plethora of constitutive modelling approaches over the decades. For instance, a typical elaborated constitutive model based on the original critical state framework [1], e.g., the cross-anisotropy model [2], requires up to 21 variables, as cited by Wood [3,4]. Adopting these complex constitutive models in numerical modelling and applying the results in practical engineering design requires a skilful geotechnical engineer to build advanced finite element models and predict the responses of soils on site or in advance. Recently, a 'strength mobilisation framework' [5–7] was proposed. It is a relatively simple empirical framework that has been proven to be applicable in estimating the mobilised stress–strain responses of hundreds of natural clays and silt when shearing in a short-term, undrained manner. This

Academic Editor(s): Grigorios Tsinidis

Received: 11 November 2024
Revised: 06 May 2025
Accepted: 23 May 2025
Published: date

Citation: Cheng, Y.P.; Liu, J.; Deng, M. Strength Mobilisation in Karlsruhe Fine Sand. *Geotechnics* **2025**, *5*, x. https://doi.org/10.3390/xxxxx

framework has also been applied to predict the level of deformation of some specific geotechnical structures, e.g., retaining walls [8,9], deep excavations [10] and bored piles [11].

Previous investigations undertaken by Vardanega and Bolton [5] were related to clay shearing in undrained conditions. Compared with undrained clays, it is uncommon for sands to be subjected to undrained shearing conditions, although loose sand can potentially liquefy [12,13]. In this case, pore pressure rises, and effective stress decreases. When the effective stress is zero, the shear capacity of the soil disappears completely, and the soil liquefies [13]. It is, however, more common for sand to be sheared under drained conditions due to its high permeability. It is therefore necessary for researchers to investigate the strength mobilisation framework for sands under drained shearing. The peak shear strength of sand depends on the grading of the sand, the confining stress level, the relative density, and the crushing strength statistics of the sand particles [14,15]. To date, few investigators have explored the strength mobilisation framework of sands. For examples, what are the curve-fitting parameters for the power-law relationship between mobilisation strength and shear strain in sands, what does the reference shear strain of sands depend on, and what are the limitations involved.

This paper attempts to explore the strength mobilisation framework of sands, mainly based on drained triaxial tests on Karlsruhe Fine Sand from a public database [16]. One purpose of this study is to assess whether the previously published mobilisation framework for clays and silt is also applicable to sands. The second purpose is to quantify the relationship between volumetric parameters and mobilised strength, as well as the stiffness of sands and the reference strain, by normalisation and regression analysis.

2. Materials and Methods

The main workflow for the data of the project is illustrated in Figure 1.

2.1. Data Collection

Three relatively different sand types were chosen to check the proposed strength mobilisation framework's applicability to sands.

Figure 2a shows that the average grain diameter for Karlsruhe Fine Sand, from Karlsruhe in southwest Germany, is 0.14 mm. The coefficient of uniformity of 1.5 indicates that the sand particles were not well graded. The particle shape is subangular, as shown in the optical microscope image in Figure 2b. T. Wichtmann and T. Triantafyllidis [16] conducted 25 monotonic triaxial tests under isotopic consolidation. The samples used had various relative densities I_D, ranging from 0.15 to 0.95. All tests can be divided into five groups for different densities (see Table 1, TMD1-TMD25), where the applied effective confining pressures are 50, 100, 200, 300 and 400, respectively.

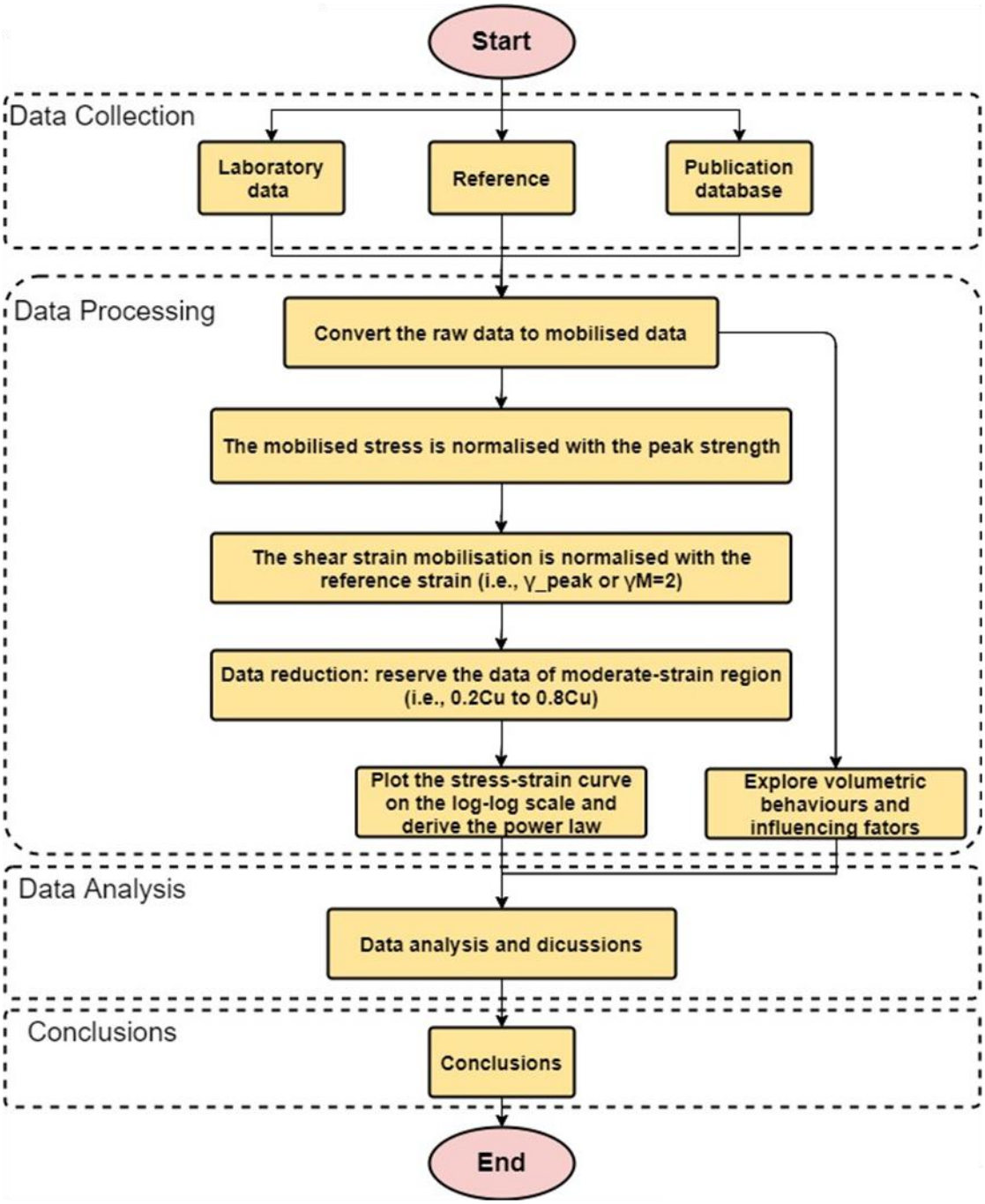

Figure 1. Flowchart diagram for the workflow of the project.

Additional data pertaining to drained triaxial tests of Clean Ottawa Sand and Fontainebleau Sand [17,18] were collected (See Table 1). This study involved two sets of triaxial test data on Ottawa sand from Ottawa in Canada (see Table 1, A14 and A17). The particle shape of this sand is rounded [19]. We also used three sets of triaxial test data of Fontainebleau Sand from south Paris in France (see Table 1, Test 3, Test 5, Test 7) [20]. This sand is weaker than Ottawa and Karlsruhe fine sand.

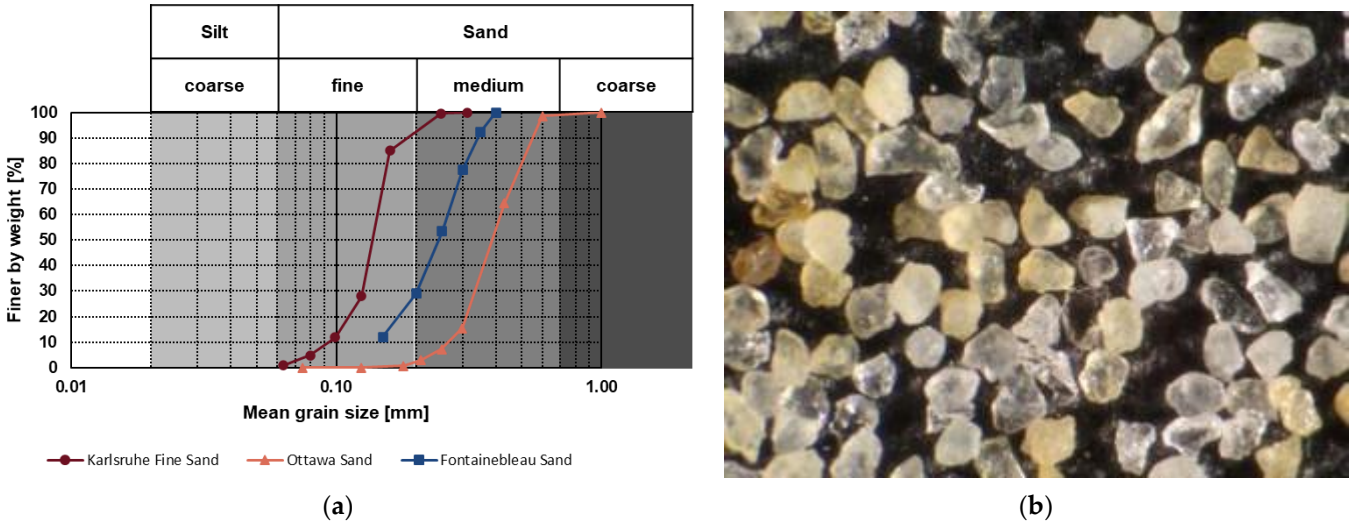

(**a**) (**b**)

Figure 2. Characteristics of sands. (**a**) Grain size distribution curve for three sands; (**b**) particle shape of grains of Karlsruhe Fine Sand with an optical microscope [16]**.** Reprinted with permission from T. Wichtmann.

Table 1. Monotonic drained triaxial tests [16–18].

Test No.	Void Ratios	Relative Densities	Effective Confining Pressures [KPa]
TMD1	0.996	0.15	50
TMD2	0.975	0.21	100
TMD3	0.975	0.21	200
TMD4	0.970	0.22	300
TMD5	0.960	0.25	400
TMD6	0.880	0.46	50
TMD7	0.862	0.51	100
TMD8	0.859	0.52	200
TMD9	0.848	0.55	300
TMD10	0.847	0.55	400
TMD11	0.840	0.57	50
TMD12	0.819	0.63	100
TMD13	0.824	0.63	200
TMD14	0.822	0.64	300
TMD15	0.814	0.68	400
TMD16	0.743	0.82	50
TMD17	0.758	0.79	100
TMD18	0.748	0.81	200
TMD19	0.734	0.85	300
TMD20	0.753	0.8	400
TMD21	0.734	0.85	50
TMD22	0.735	0.85	100
TMD23	0.706	0.92	200
TMD24	0.697	0.95	300
TMD25	0.718	0.89	400
A14 Ottawa	0.558	0.74	100
A17 Ottawa	0.699	0.27	400
Test 3-CID Fontainebleau	0.684	0.57	200
Test 5-CID Fontainebleau	0.660	0.65	100
Test 7-CID Fontainebleau	0.612	0.80	50

2.2. Data Reduction and Processing

The originally divergent stress–strain curves of London clay before normalisation are shown in Figure 3 as an example, where the legend represents different samples. The solid and hollow triangles denote the reference strain γ_{ref} corresponding to $\gamma_{M=2}$ (shear strain at half peak undrained strength $C_u/2$) and γ_{peak} (shear strain at peak undrained shear strength C_u), respectively. For further analysis, the *Y*-axis can be expressed as normalised strength mobilisation ratio *M*, which is defined as the mobilized shear strength τ_{mob} over the undrained shear strength C_u, i.e., τ_{mob}/C_u, and the *X*-axis can be expressed as mobilised shear strain normalised by a reference strain, i.e., γ/γ_{ref}. Note that only the moderate strength region between $0.2C_u$ and $0.8C_u$ is considered, because both high-strength ($> 0.8C_u$) and low-strength ($< 0.2C_u$) regions are not typically needed for the design purpose. If the soil shear strength was designed to be greater than $0.8C_u$, the structure would be too close to failure and unsafe. In contrast, if it was assumed to be less than $0.2C_u$, the structure would be unnecessarily safe and too expensive to build. The results obtained from the moderate-strength region, however, reveal a unified stress–strain curve that could be approximated by a power–law function [6,7].

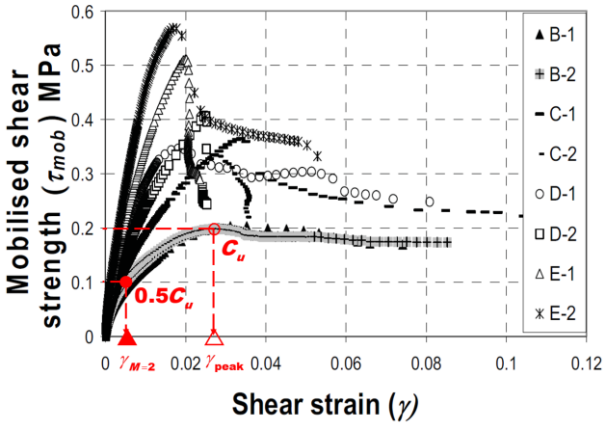

Figure 3. Mobilised shear stress-strain curves of London clay from Yimsiri (2001) [6]. Reprinted with permission from P. J. Vardanega.

In order to correctly analyse the drained shearing data of sands, the mobilised shear stress τ_{mob} and mobilised shear strain γ_{mob} need to be calculated accurately in the axisymmetric system of triaxial testing. In undrained shearing, shear strain is given by $\gamma = 1.5\varepsilon_a$. However, the coefficient of 1.5 in [5] is unsuitable for drained conditions. The shear strain equals to axial strain ε_a minus radial strain, which can be expressed as the product of Poisson's ratio and axial strain based on Hooke's Law. In undrained conditions, the soil sample volume remains constant, resulting in a Poisson's ratio of 0.5 (see Appendix A). However, sand's peak strength is difficult to reach in undrained cases, but would be found in drained cases. Due to the changeable volume in drained conditions, Poisson's ratio is less than 0.5. Evidence summarized by K. Yokota and M. Konno [21] indicate that Poisson's ratio for sands in drained conditions is around 0.3. Therefore, the coefficient of 1.5 in [5] should be modified to 1.3, as shown in Equation (1). Equation (2) is valid for both drained and undrained triaxial shearing conditions, where the deviator stress q is the difference between major and minor principal stresses. Hence $0.5q$ is the mobilised shear stress τ_{mob}.

$$\gamma_{mob} = 1.3\varepsilon_a, \quad (1)$$

$$\tau_{mob} = 0.5q, \quad (2)$$

Using Equations (1) and (2) to convert the deviator stresses and axial strains to mobilised stresses and mobilised strains, geotechnical engineers could monitor shear strain in real time regarding the stress–strain curve [5]. The *Y*-axis in the normalised plot is τ_{mob} over τ_{peak}, and the *X*-axis is γ_{mob} over reference strain γ_{ref}. The reference strain could be either the strain at peak shear stress γ_{peak} or at half of the peak shear stress $\gamma_{M=2}$.

The normalising process changes the variables into a dimensionless range between zero and one, facilitating data processing. Note that Vardanega and Bolton [5] mentioned that when shear stress is normalised with the undrained shear strength, the effect of anisotropy is automatically filtered out in the correlation.

When using hyperbolas, it is difficult to obtain unknown parameters from the relationship directly, e.g., parameter α in Equation (3) below [22]:

$$\frac{G}{G_{max}} = \frac{1}{1 + \left(\frac{\gamma}{\gamma_{ref}}\right)^{\alpha}} \quad (3)$$

Hence, Equation (3) could be transformed to facilitate analysis. Firstly, we switch the numerators and denominators on both sides of the equation to convert the correlation to a power function. The variable is then isolated by rearranging terms, and logarithms are taken of both sides:

$$\log_{10}\left(\frac{G_{max}}{\mathrm{G}} - 1\right) = \log_{10}\left(\frac{\gamma}{\gamma_{ref}}\right)^{\alpha} \quad (4)$$

Apply the power rule to drop down the exponent:

$$\log_{10}\left(\frac{G_{max}}{\mathrm{G}} - 1\right) = \alpha \cdot \log_{10}\left(\frac{\gamma}{\gamma_{ref}}\right) \quad (5)$$

In theory, all transformed hyperbolas pass through the origin when $\gamma = \gamma_{M=2}$. When γ_{peak} is taken as the reference strain, Equation (5) would be transformed to Equation (6). But there is no reference to verify the reliability of the regression analysis.

$$\log_{10}\left(\frac{G_{max}}{\mathrm{G}} - 1\right) = \alpha \cdot \log_{10}\left(\frac{\gamma}{\gamma_{peak}}\right) + C \quad (6)$$

Hence, the stiffness reduction function can be written as:

$$\frac{G}{G_{max}} = \frac{1}{1+10^{C.}\left(\frac{\gamma}{\gamma_{peak}}\right)^{\alpha}}, \quad (7)$$

2.3. Data Analysis

Within the strength mobilisation framework for clays [5], the power curves show that the stress–strain response forms a straight line on log-log plots.

Subsequently, regression analysis served as the principal methodology in this research to quantitatively simulate the relationship between variables and develop statistical models for predicting relevant geotechnical parameters. Vardanega and Bolton [5] presented a power–law relationship between normalised mobilisation stress and strain. Hence, normalised data are plotted on log-log graphs to clarify this linear relationship. However, the reliability of results depends on both the quantity and quality of data. The coefficient of determination R^2 indicates fitting quality, with values closer to unity denoting better fit. Meanwhile, data volume also has an impact on the results.

In contrast, previous studies indicate that the stiffness–strain relationship follows a hyperbolic model [23].

3. Results

3.1. Predicting Mobilisation Strain

The results of the mobilised stress–strain relationships are presented in Figure 4. The power law function for Karlsruhe fine sand using γ_{peak} as the reference strain is:

$$\frac{\tau_{mob}}{\tau_{peak}} = 1.61\left(\frac{\gamma}{\gamma_{peak}}\right)^{0.52} \quad (8)$$

Figure 5 provides the mobilised stress–strain relationships using $\gamma_{M=2}$ as the reference strain. The resulting regression for Karlsruhe fine sand in this case is:

$$\frac{\tau_{mob}}{\tau_{peak}} = 0.48\left(\frac{\gamma}{\gamma_{M=2}}\right)^{0.52} \quad (9)$$

The choice of reference strain has no impact on the exponent, which is the crucial parameter for mobilisable strength design (MSD). However, using $\gamma_{M=2}$ as the reference strain makes it easier for investigators to verify the derived equation. The existing database also indicates that $\gamma_{M=2}$ yields slightly better correlation than γ_{peak}.

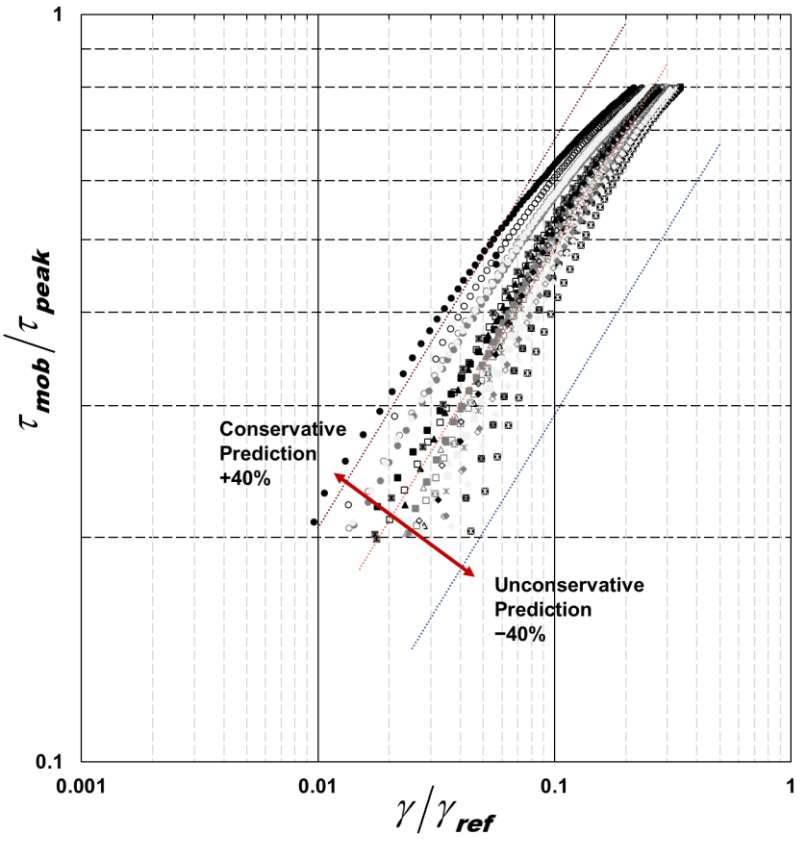

(**a**)

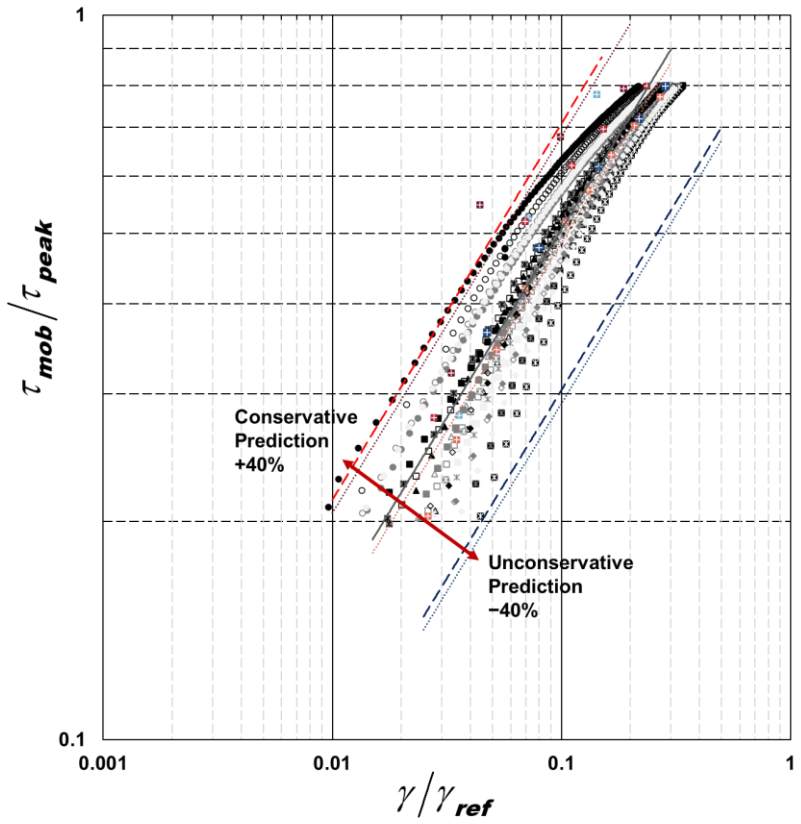

(**b**)

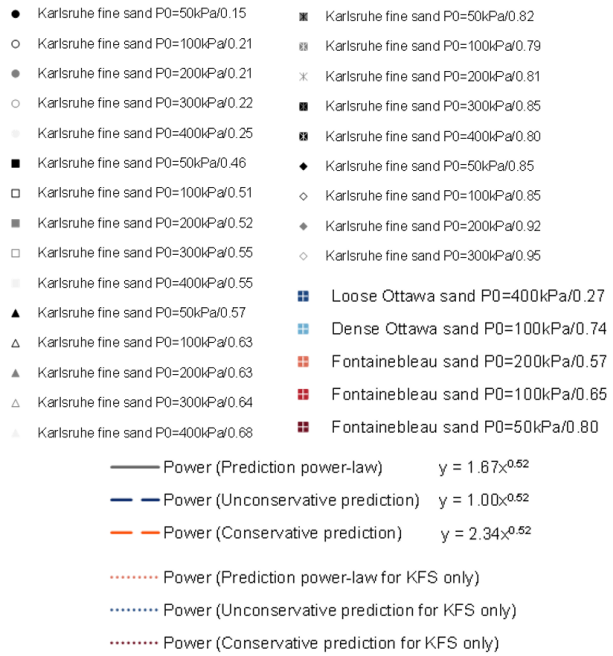

(**c**)

Figure 4. Mobilised stress-strain curves for 30 triaxial tests (γ_{peak}). (**a**) Karlsruhe fine sand only; (**b**) three sands including Karlsruhe fine sand (all grey); (**c**) legend.

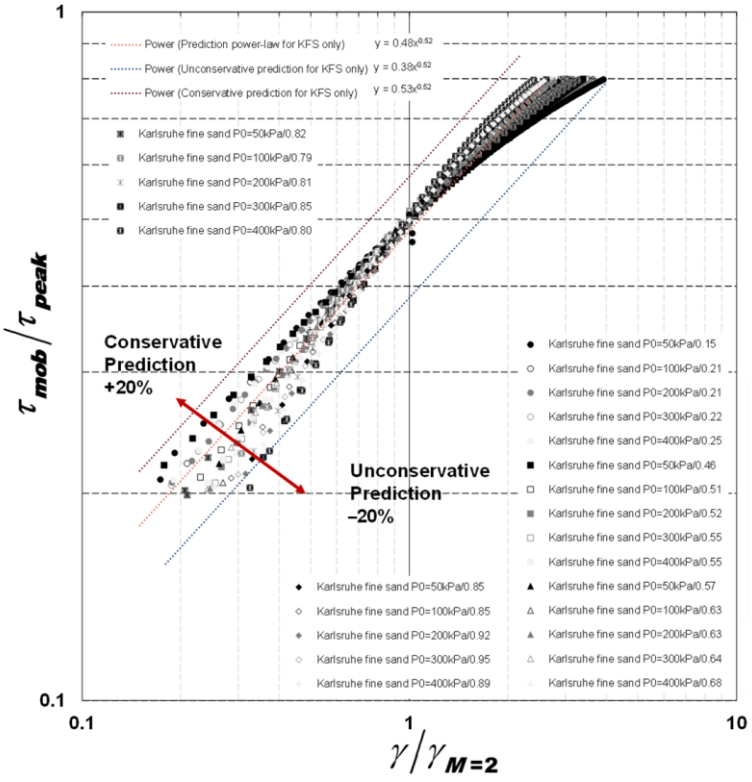

(**a**)

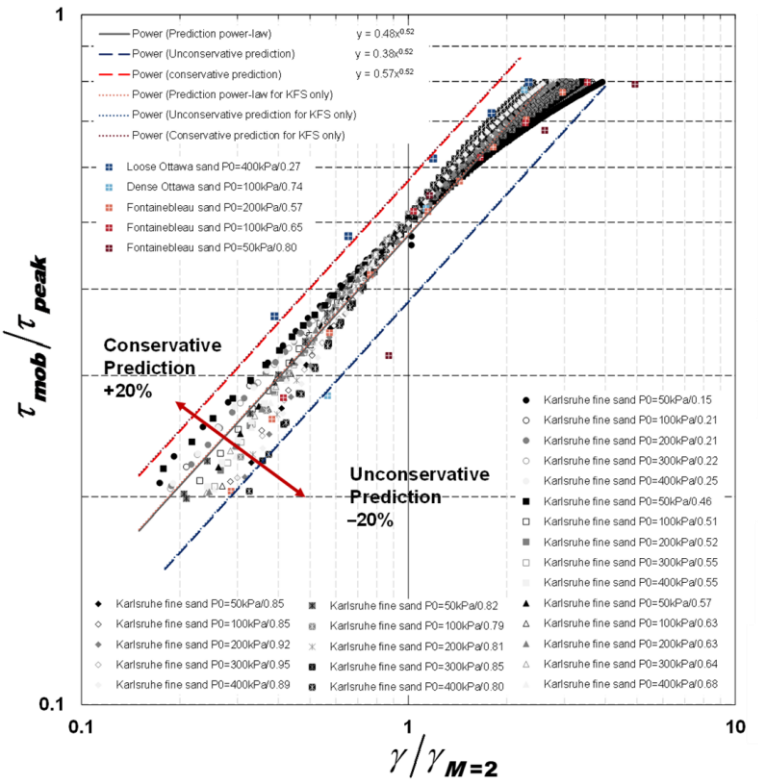

(**b**)

Figure 5. Mobilised stress–strain curves for 30 triaxial tests ($\gamma_{M=2}$). (**a**) Karlsruhe fine sand only; (**b**) three sands including Karlsruhe fine sand (all grey).

The value of the exponent for sands (0.52) is lower than that for clays (0.6). This means that at the same stress mobilisation ratio, say $\tau_{mob}/\tau_{peak} = 0.8$, the value of normalised shear strain for sands is higher than that for clays (see Figure 6). In other words, the

deformation of sands relative to the reference shear strain $\gamma_{M=2}$ could be slightly larger than that of clays at the same moblised stress level exceeding $0.5\tau_{peak}$. The error range for sands (0.9 to 1.7) is narrower than that for clays (0.57 to 1.75), which indicates a better result (see Figure 6). Note that only one type of sand is considered here, whereas previous published data for clay consisted of a much larger dataset from around the world.

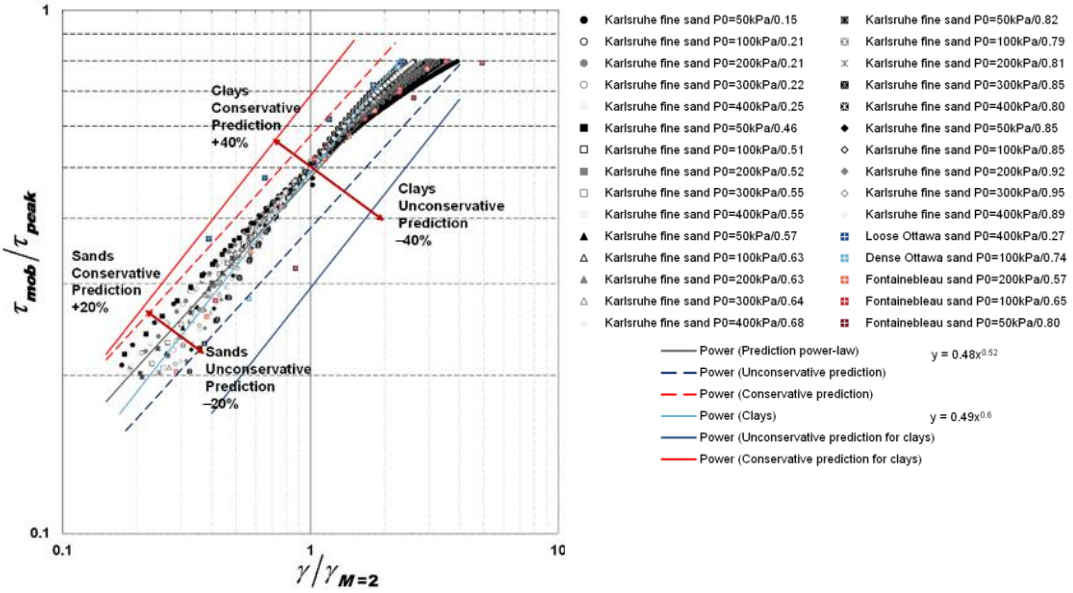

Figure 6. A comparison of power laws between sands and clays.

3.2. Sand Behaviours

Figure 7 shows the locations of the reference shear strains for different groups of relative density (RD). When the relative density of samples increases at the same confining stress level, the shear strength increases and the reference strain decreases. For low relative densities (RD = 0.15–0.25), peak shear strength occurs at large deformation (γ_{ref} = 0.3). The reference shear strength decreases from around 0.3 to less than 0.1 when RD is at the highest of around 0.79–0.85.

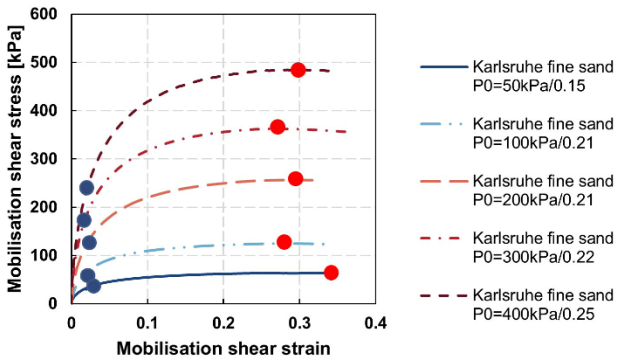

(**a**)

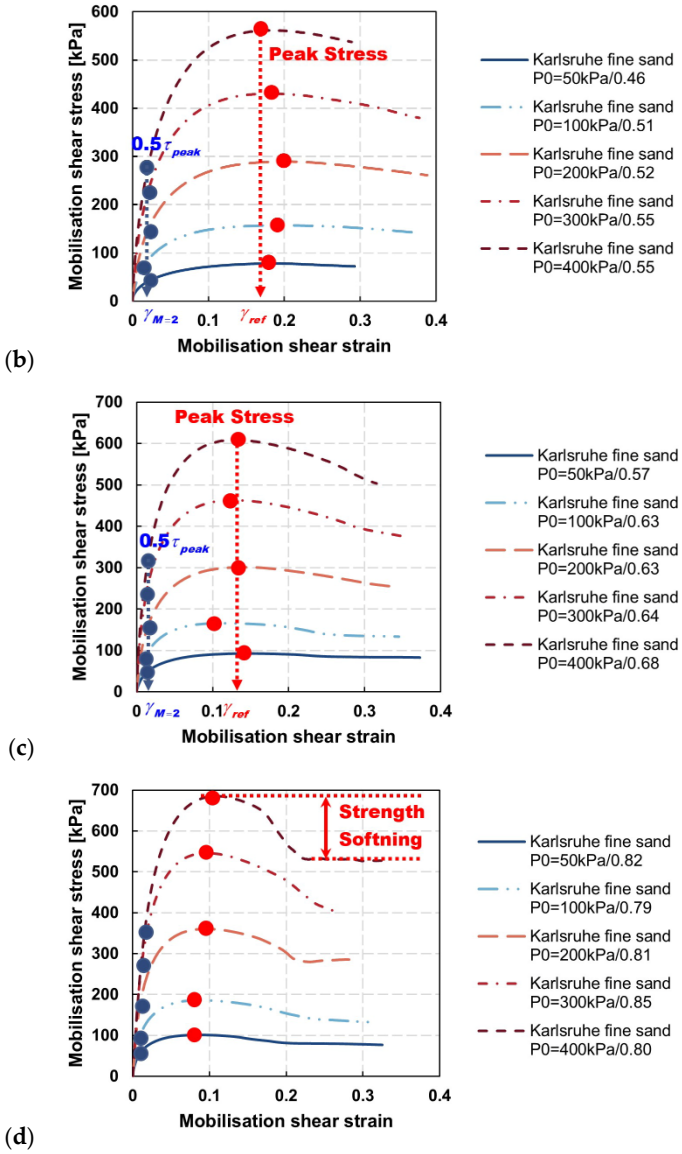

Figure 7. Stress–strain curves for sands with various confining pressures ranging from 100 to 400 kPa and relative densities ranging from (a) 0.15 to 0.25; (b) 0.46 to 0.55; (c) 0.57 to 0.68; and (d) 0.79 to 0.85.

Figure 8b presents the volumetric behaviour for sands, which shows initial contraction (with positive volumetric strain) followed by dilation. Notably, actual critical states were not reached in these tests, especially under lower confining pressure.

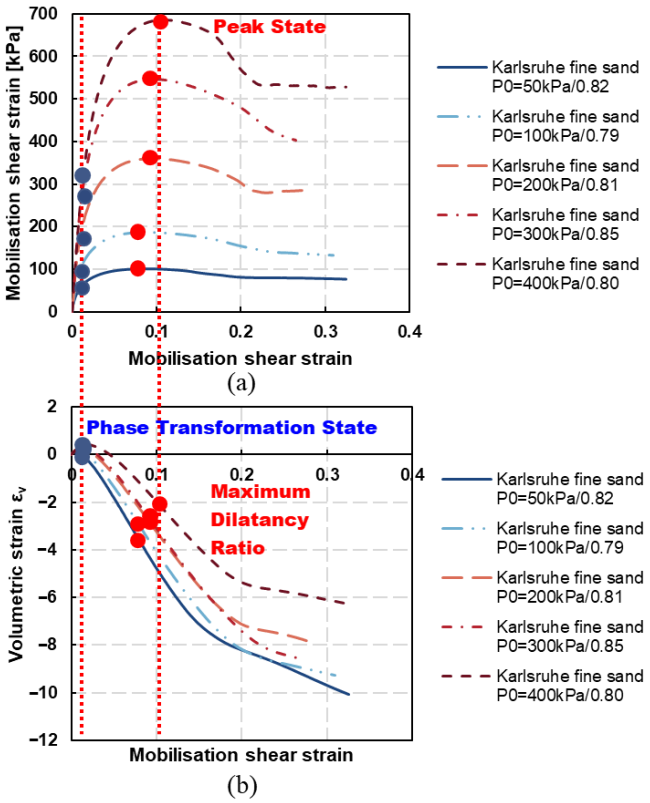

Figure 8. An example of sand behaviours under various confining pressures and relative densities: (a) mobilisation shear stress versus mobilisation shear strain; (b) volumetric strain versus mobilisation shear strain.

Figure 9 represents the stress–dilatancy behaviour of a Karlsruhe fine sand specimen under drained loading. The stress ratio is $\eta=q/p'$, where q is the deviator stress and p' is the effective mean stress. Dilatancy is defined as $D=d\varepsilon_v/d\gamma$ (the slope in Figure 8b). Figure 9 shows that both phase transformation and final critical states occur at consistent stress ratios of around 0.4 and 1.4, respectively, regardless of the initial sample's relative density. At the beginning of shearing, the sand goes through strain hardening and volumetric contraction. After the phase transformation state, dilatancy occurs. The peak state occurs subsequently at the maximum dilatancy ratio (D_{max}). Strength softening develops when volumetric dilatancy reduces after the peak state. Dilatancy reduces towards the critical state, where D = 0. This manifests a typical stress–dilatancy behaviour of soils, as proposed by Been and Jefferies [24].

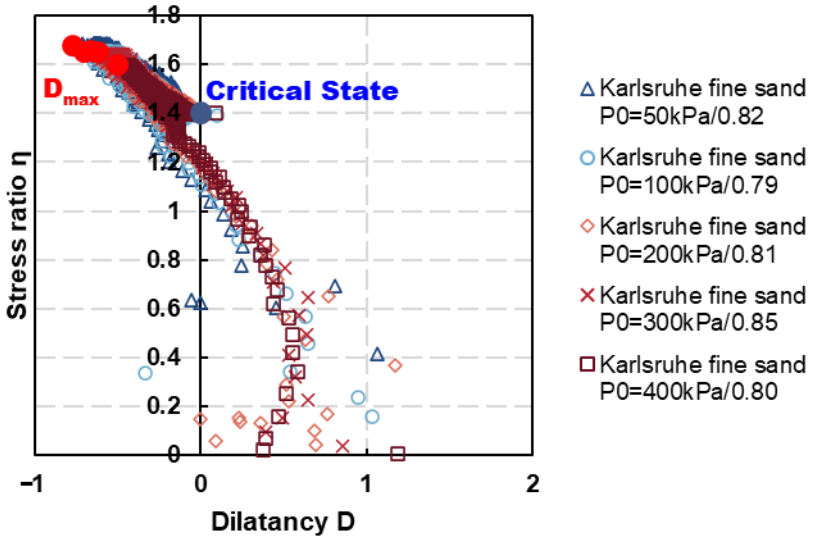

Figure 9. Examples of stress–dilatancy relationships for drained Karlsruhe Fine Sand with relative density ranging from 0.79 to 0.85.

The maximum dilatancy for denser samples (with higher relative density and lower void ratio) is higher than that of looser samples at the same confining stress levels, indicating greater volumetric dilation in denser samples. For instance, at the confining pressure of 100 kPa, the maximum dilatancy ranges from 0.1 to 0.7 across loose to dense samples. As the confining pressure increases, both the initial shear modulus and peak shear strength increase. As a result, at the same level of relative density, samples with higher confining pressure exhibit lower maximum dilatancy.

Figures 10 and 11 reveal strong linear relationships in the reference strain $\gamma_{M=2}$ between various parameters including relative density, relative dilatancy, relative dilatancy index, and stress ratio, but not confining pressure. The quantitative analyses of the relationships between two reference strains, $\gamma_{M=2}$ and γ_{peak}, and these parameters are summarised in Table 2. The results for γ_{peak} are better than those for $\gamma_{M=2}$ as they give higher R^2 values.

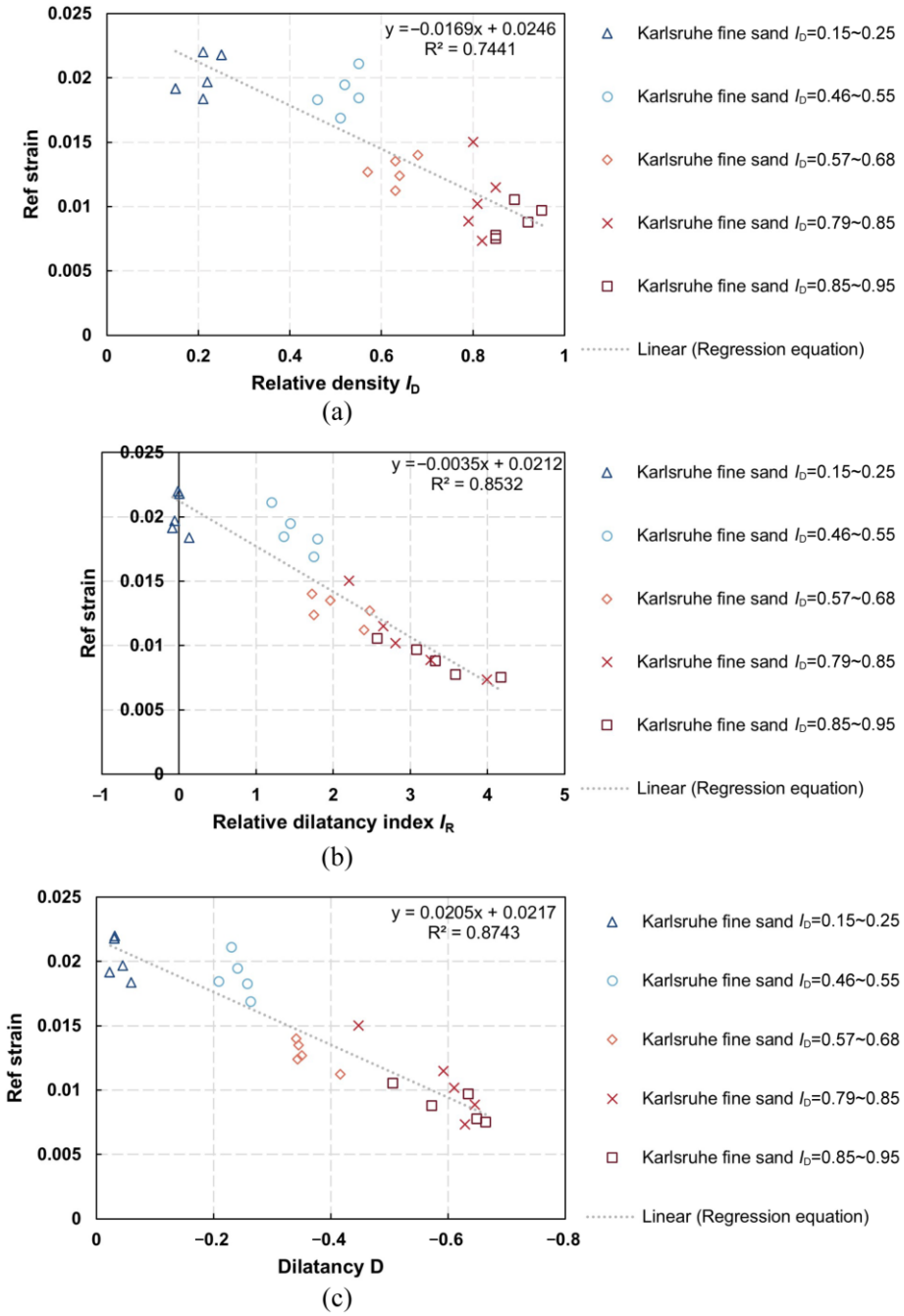

Figure 10. Quantitative analyses of the relationships between reference strain $\gamma_{M=2}$ and (a) relative density; (b) relative density index; and (c) dilatancy.

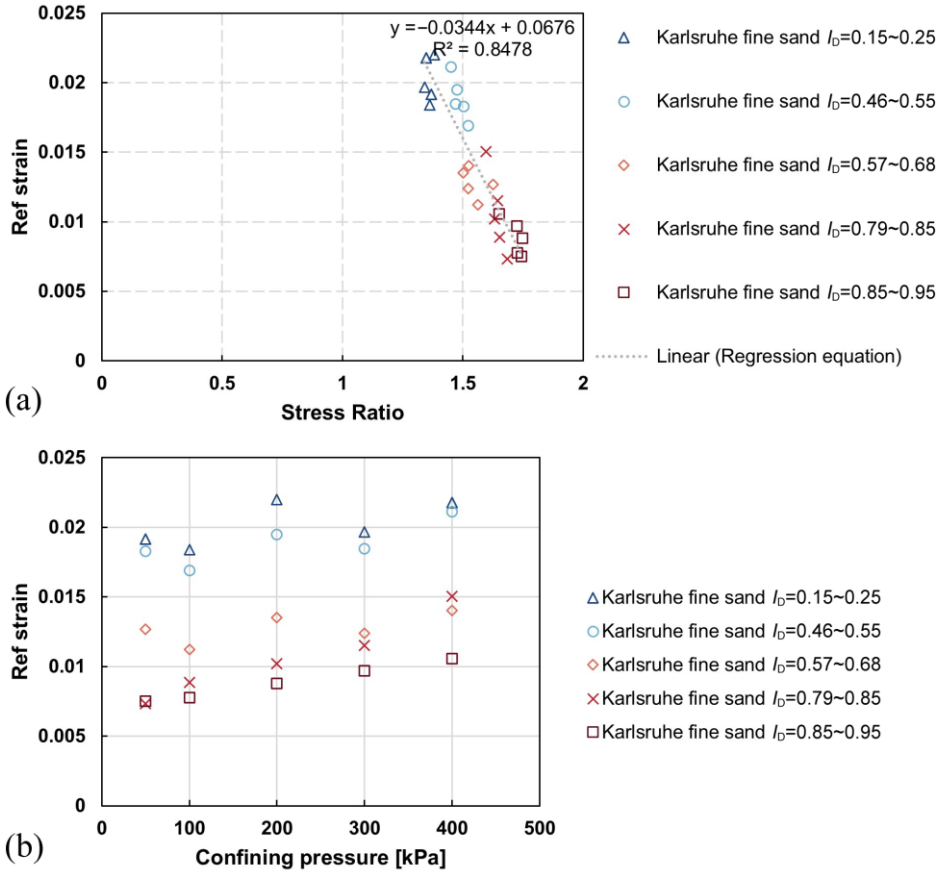

Figure 11. Quantitative analyses of the relationships between reference strain $\gamma_{M=2}$ and (a) stress ratio and (b) confining pressure.

Table 2. Quantitative analyses of the relationships between reference strain and various parameters.

Reference Strain	Relative Density	Relative Density Index	Dilatancy	Stress Ratio	Confining Pressure
$\gamma_{M=2}$	$\gamma_{M=2} = -0.017I_D + 0.025$ $R^2 = 0.74$	$\gamma_{M=2} = -0.0035I_R + 0.021$ $R^2 = 0.85$	$\gamma_{M=2} = 0.020D_{min} + 0.022$ $R^2 = 0.87$	$\gamma_{M=2} = -0.0344\eta + 0.068$ $R^2 = 0.85$	N/A
γ_{peak}	$\gamma_{peak} = -0.32I_D + 0.35$ $R^2 = 0.94$	$\gamma_{peak} = -0.060I_R + 0.28$ $R^2 = 0.87$	$\gamma_{peak} = 0.35D_{min} + 0.29$ $R^2 = 0.89$	$\gamma_{peak} = -0.57\eta + 1.047$ $R^2 = 0.85$	N/A

Figure 12 demonstrates the relationship between the dilatancy rate and relative density, along with the relative dilatancy index. The dilatancy rate is well correlated with the relative dilatancy index. However, the slope of the best fit line in Figure 12 is 0.22 for Karlsruhe fine sand, which is lower than the 0.31 proposed by Bolton [14]. This difference might be attributed to the soil type.

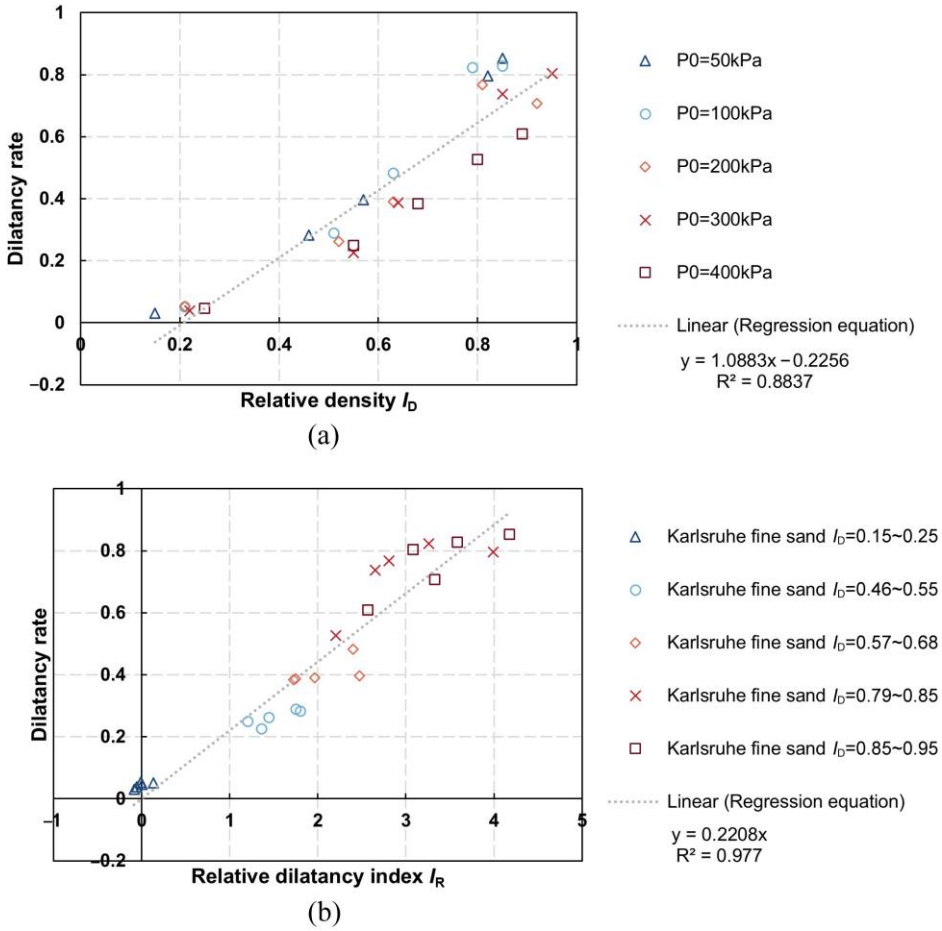

Figure 12. Dilatancy rate versus (a) relative density and (b) relative dilatancy index for drained Karlsruhe fine sand with various confining pressures and relative densities.

Figure 13 provides the results for Karlsruhe fine sand at peak strength with relative density ranging from loose to dense. The maximum stress ratio for the densest sample is around 1.7. The linear regression equation derived from these data is as follows:

$$\eta_{max} = -0.56 \times D_{min} + 1.34, \; R^2 = 0.93 \quad (10)$$

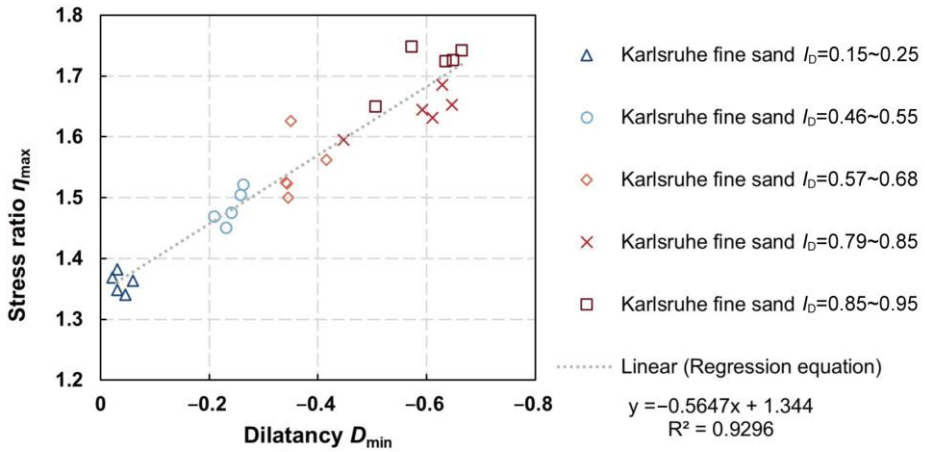

Figure 13. η_{max}–D_{min} relationship for Karlsruhe fine sand ranging from loose to dense at low confining pressures in triaxial tests.

The hyperbola describing the relationship between normalised shear modulus and normalised mobilisation strain (See Figure 14) is given by

$$\frac{G}{G_{max}} = \frac{1}{1+35.8\times(\frac{\gamma}{\gamma_{peak}})^{0.87}},\ R^2 \approx 0.97 \quad (11)$$

$$\frac{G}{G_{max}} = \frac{1}{1+(\frac{\gamma}{\gamma_{M=2}})^{0.87}},\ R^2 \approx 0.89 \quad (12)$$

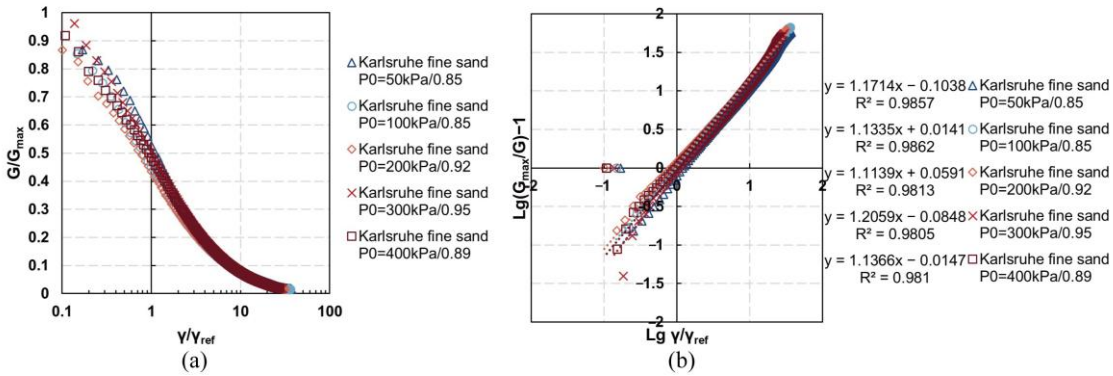

Figure 14. (a) An example of a shear modulus reduction curve for Karlsruhe fine sand with relative density ranging from 0.85 to 0.95; (b) in logarithmic form.

The α value of 0.87 for sands is larger than the 0.74 for clays and silts reported by Vardanega and Bolton [22]. This indicates that the degradation of the normalised shear modulus for clays is gentler and smoother [25–26].

4. Discussion

The determination of Poisson's ratio under drained conditions has a significant impact on the results. An assumption of 0.3 is adopted in this research. However, Poisson's ratio for sands under drained conditions ranges from 0.2 to 0.4. A limitation of using the average value is that it may not accurately represent Poisson's ratio across different soils in the drained state. In fact, the relationship between radial strain and axial strain fits better to a straight line with a Poisson's ratio of around 0.22. This limitation can be reduced with an expanded sand database in the future. Based on the data for three sands investigated under the drained condition, the power laws are summarised in Table 3. What is interesting is that all three sands share an identical exponent of 0.52, suggesting a generalisable power law for sands. Table 4 shows data for clays from previous literatures and compares their power laws. It is found that the clays generally yield a higher exponent. Table 5 summarises the hyperbolic functions for stiffness reduction with high coefficients of determination. The exponent for sands is larger than that of clays, which means the stiffness of sands undergoes a more significant reduction than that of clays when the mobilised strain increases.

Table 3. Comparison of power laws for Karlsruhe Fine Sand with a different reference strain.

Power Law (Karlsruhe Fine Sand)	Standard Deviator	Power Law (Three Sands)	Standard Deviator
$\frac{\tau_{mob}}{\tau_{peak}} = 0.48(\frac{\gamma}{\gamma_{M=2}})^{0.52}$	0.006	$\frac{\tau_{mob}}{\tau_{peak}} = 0.48(\frac{\gamma}{\gamma_{M=2}})^{0.52}$	0.02
$\frac{\tau_{mob}}{\tau_{peak}} = 1.61(\frac{\gamma}{\gamma_{peak}})^{0.52}$	0.1	$\frac{\tau_{mob}}{\tau_{peak}} = 1.67(\frac{\gamma}{\gamma_{peak}})^{0.52}$	0.34

Table 4. Comparison of power laws fitted to Karlsruhe fine sand and different types of clays.

Soil Type	Exponent b	Std Dev	Index A	Std Dev	Error Range	Power Laws	Source
Clays	0.60	0.15	0.49	N/A	±40%	$\frac{\tau_{mob}}{C_u} = 0.49\left(\frac{\gamma}{\gamma_{M=2}}\right)^{0.6}$	[5]
London Clay	0.58	0.04	0.49	0.04	±20%	$\frac{\tau_{mob}}{C_u} = 0.49\left(\frac{\gamma}{\gamma_{M=2}}\right)^{0.58}$	[6]
Kaolin Clay	N/A	N/A	0.50	N/A	±40%	N/A	[7]
Sands $\gamma_{M=2}$	0.52	0.07	0.48	0.02	±20%	$\frac{\tau_{mob}}{\tau_{peak}} = 1.61(\frac{\gamma}{\gamma_{peak}})^{0.52}$	This Project
Sands γ_{peak}	0.52	0.07	1.67	0.34	±40%	$\frac{\tau_{mob}}{\tau_{peak}} = 0.48(\frac{\gamma}{\gamma_{M=2}})^{0.52}$	This Project

Table 5. Comparison of relationships between shear modulus reduction with normalised shear strain for clays and Karlsruhe fine sand with a reference strain of $\gamma_{M=2}$.

Soil Type	Function	R^2	Source
Clays $\gamma_{M=2}$	$\frac{G}{G_{max}} = \frac{1}{1+(\frac{\gamma}{\gamma_{ref}})^{0.74}}$	0.95	[22]
Clays $\gamma_{M=2}$	$\frac{G}{G_{max}} = \frac{1}{1+(\frac{\gamma}{\gamma_{ref}})^{0.74}}$	0.96	[25]
Karlsruhe Fine Sand $\gamma_{M=2}$	$\frac{G}{G_{max}} = \frac{1}{1+(\frac{\gamma}{\gamma_{ref}})^{0.87}}$	0.89	This Project

5. Conclusions

This research represents the first exploration of the strength mobilisation framework for sands. Based on drained triaxial test data of three sands, it is shown that the framework proposed for clay and silts by Vardanega and Bolton [5] remains applicable to sands.

(1) A power function relating normalised shear stress and shear stain $\frac{\tau_{mob}}{\tau_{peak}} = 0.48\left(\frac{\gamma}{\gamma_{M=2}}\right)^{0.52}$ was obtained in the moderate stress region of 0.2 to 0.8 of peak shear stress τ_{peak}. The exponent for sands (0.52) is lower than that of clays, indicating that in general, clay mobilises its strength faster than sands in a normalised sense. However, the exact magnitude of the reference strain of each sand sample is different, and clays generally have a larger reference strain than sands. Using $\gamma_{M=2}$ as the reference strain gives a slightly better fitting than γ_{peak}, with errors within the acceptable range of +/−20% for the sands investigated.

(2) The reference shear strain reveals strong linear relationships with dilatancy-related parameters, such as relative density and relative dilatancy index, but not directly with confining pressure.

(3) There is a hyperbolic function fitting the relationship between normalised shear modulus and normalised mobilisation strain. The fitting coefficient α is 0.87 for sands, compared to the 0.74 for clays and silts proposed by Vardanega and Bolton [22].

(4) This research confirms that a simple empirical power–law stress–strain function can potentially be used by engineers to predict sand deformation with structures built on it. The function derives directly from triaxial test data without the need for plastic potential theory to predict strain. Future work should focus on expanding the database and validating the approach through case studies.

Author Contributions: J.L.: formal analysis, data interpretations, writing—original draft. Y.P.C.: supervision. M.D.: review and editing—original draft. All authors have read and agreed to the published version of the manuscript.

Funding: No fundings.

Data Availability Statement: Published data were adopted.

Acknowledgments: The authors would like to acknowledge Wichtmann Torsten for the database he produced with his co-workers. Appreciations are extended to Choi Lin Chan for her helpful advice.

Conflicts of Interest: The authors declare no conflicts of interest.

Appendix A

Suppose the lengths of the three sides of the rectangular micro-element are x, y and z, and the deformations for each side are dx, dy and dz, respectively.

$$\text{Volume before the change: } V_1 = xyz.$$

$$\text{Volume after the change: } V_2 = (x + \mathrm{d}x)(y + \mathrm{d}y)(z + \mathrm{d}z).$$

$$\text{Volume change: } \mathrm{dV} = V_2 - V_1.$$

Neglecting the higher-order term, the volume strain is:

$$\frac{\mathrm{d}V}{V_1} = \frac{V_2 - V_1}{V_1} \approx \frac{(yz \cdot \mathrm{d}x + xz \cdot \mathrm{d}y + xy \cdot \mathrm{d}z)}{xyz}$$

$$\frac{\mathrm{d}V}{V_1} = \frac{\mathrm{d}x}{x} + \frac{\mathrm{d}y}{y} + \frac{\mathrm{d}z}{z} = \varepsilon xx + \varepsilon yy + \varepsilon zz$$

$$\because \varepsilon yy = \varepsilon zz = -\mu \cdot \varepsilon xx \ (\mu \ is \ Poisson's \ ratio)$$

$$\therefore \frac{\mathrm{d}V}{V_1} = (1 - 2\mu)\varepsilon xx$$

References

1. Roscoe, K.H.; Burland, J.B. On the generalised stress-strain behaviour of wet clay. *Eng. Plast*. **1968**, 535–609. https://www.researchgate.net/publication/264921746_On_the_Generalized_Stress-Strain_Behavior_of_Wet_Clays
2. Graham, J.; Houlsby, G.T. Anisotropic elasticity of a natural clay. *Géotechnique* **1983**, *33*, 165–180.
3. Wood, D.M. Elasticity. In *Soil Behaviour and Critical State Soil Mechanics*; Cambridge University Press: Cambridge, UK, 1991; pp. 37–54.
4. Wood, D.M. Elastic-plastic modelfor soil. In *Soil Behaviour and Critical State Soil Mechanics*; Cambridge University Press: Cambridge, UK, 1991; pp. 84–111.
5. Vardanega, P.J.; Bolton, M.D. Strength mobilization in clays and silts. *Can. Geotech. J.* **2011**, *48*, 1485–1503.
6. Yimsiri, S. Pre-Deformation Characteristics of Soils: Anisotropy and Soil Fabric. Ph.D. Thesis, University of Cambridge, Cambridge, UK, 2001.
7. Vardanega, P.J.; Lau, B.H.; Lam, S.Y.; Haigh, S.K.; Madabhushi, S.P.G.; Bolton, M.D.; Mayne, P.W. Discussion: Laboratory measurement of strength mobilisation in kaolin: Link to stress history. *Geotech. Lett.* **2013**, *3*, 16–17.
8. Osman, A.S.; Bolton, M.D. A new design method for retaining walls in clay. *Can. Geotech. J.* **2004**, *41*, 451–466.
9. Deng, C.; Haigh, S.K.; Ma, X.; Xu, J. A design method for flexible retaining walls in clay. *Geotechnique* **2021**, *71*, 178–187.
10. Lam, S.Y.; Bolton, M. Energy Conservation as a Principle Underlying Mobilizable Strength Design for Deep Excavations. *J. Geotech. Geoenvironmental Eng.* **2011**, *137*, 1062–1074.
11. Vardanega, P.J.; Williamson, M.G.; Bolton, M.D. Bored pile design in stiff clay II: Mechanisms and uncertainty. *Proc. Inst. Civ. Eng. Geotech. Eng.* **2012**, *165*, 233–246.
12. Vasko, A. *An Investigation into the Behavior of Ottawa Sand through Monotonic and Cyclic Shear Tests*; The George Washington University: Washington, DC, USA, 2015.
13. Atigh, E.; Byrne, P.M. Flow Liquefaction Failure of Submarine Slopes Due to Monotonic Loadings—An Effective Stress Approach. In *Submarine Mass Movements and Their Consequences: 1st International Symposium*; Locat, J., Mienert, J., Boisvert, L., Eds.; Springer Netherlands: Dordrecht, The Netherlands, 2003; pp. 3–10.
14. Bolton, M.D. The strength and dilatancy. *Geotechnique* **1986**, *36*, 65–78.
15. Dong, Z.; Tong, C.; Zhang, S.; Cheng, Y.P.; Sheng, D. Strength and Dilatancy of Crushable Soils with Different Gradings. *Can. Geotech. J.* **2024**, *62*, 1–21.
16. Wichtmann, T.; Triantafyllidis, T. An experimental database for the development, calibration and verification of constitutive models for sand with focus to cyclic loading: Part I—Tests with monotonic loading and stress cycles. *Acta Geotech.* **2016**, *11*, 739–761.
17. Salgado, R.; Bandini, P.; Karim, A. Shear Strength and Stiffness of Silty Sand. *J. Geotech. Geoenvironmental Eng*. **2000**, *126*, 451–462.
18. Latini, C.; Zania, V. *Triaxial Tests in Fontainebleau Sand*; Technical University of Denmark Internal Report; Technical University of Denmark: Kongens Lyngby, Denmark, 2017.
19. Erdoğan, S.T.; Forster, A.M.; Stutzman, P.E.; Garboczi, E.J. Particle-based characterization of Ottawa sand: Shape, size, mineralogy, and elastic moduli. *Cem. Concr. Compos.* **2017**, *83*, 36–44.
20. Al Saadi, F.; Wolf, K.-H.; van Kruijsdijk, C. Characterization of Fontainebleau Sandstone: Quartz Overgrowth and its Impact on Pore-Throat Framework. *J. Pet. Environ. Biotechnol*. **2017**, *8*, 1–12.
21. Yokota, K.; Konno, M. Dynamic Poisson's ratio of soil. In Proceedings of 7th World Conference Earthquake Engineering Istanbul, Istanbul, Turkey, 8–13 September 1980; Volume 3, pp. 475–478.
22. Vardanega, P.J.; Bolton, M.D. Stiffness of Clays and Silts: Normalizing Shear Modulus and Shear Strain. *J. Geotech. Geoenvironmental Eng.* **2013**, *139*, 1575–1589.
23. Oztoprak, S.; Bolton, M.D. Stiffness of sands through a laboratory test database. *Geotechnique* **2013**, *63*, 54–70.
24. Been, K.; Jefferies, M. Stress-dilatancy in very loose sand. *Can. Geotech. J.* **2004**, *41*, 972–989.
25. Vardanega, P.J.; Bolton, M.D. Practical methods to estimate the non-linear shear stiffness of fine grained soils. In *Deformation Characteristics of Geomaterials*; IOS Press: Amsterdam, The Netherlands 2011; pp. 372–379.
26. Vardanega, P.J.; Bolton, M. Stiffness of Clays and Silts: Modeling Considerations. *J. Geotech. Geoenvironmental Eng.* **2014**, *140*, 6014004.